

MOLECULAR CHARACTERIZATION AND EXPRESSION ANALYSIS OF *DoVIN2* IN *DENDROBIUM OFFICINALE* UNDER COLD AND DROUGHT STRESS

BOTING LIU^{1,2†}, XIANG LI^{1,2†}, YANPING WU², YINGZHI ZHANG³, YONG ZHANG²,
YUANLONG LIU⁴, JIE CHEN^{1,2*} AND YUJIA LIU^{1,2*}

¹Guangdong Province key Laboratory of Utilization and Conservation of Food and Medicinal Resources in Northern Region, Shaoguan University, Shaoguan 512005, China

²College of Biology and Agriculture, Shaoguan University, Shaoguan 512005, China

³School of Food, Shaoguan University, Shaoguan 512005, China

⁴State Key Laboratory for Conservation and Utilization of Subtropical Agro-Bioresources, South China Agricultural University, Guangzhou 510642, China Pakistan

*Corresponding author's liuyj1206@sgu.edu.cn

Abstract

Sucrose metabolism is a crucial metabolic process in plants that involves acid invertase. Nonetheless, the precise function and structural characteristics of the vacuolar invertase (VINV) gene in *Dendrobium officinale* (*D. officinale*) remain unclear. In this study, the putative vacuolar invertase gene (*DoVIN2*) was isolated from the DanXia cultivar using homologous cloning techniques. *DoVIN2* exhibited a cDNA sequence spanning 1368 bp, encoding a protein consisting of 455 amino acids with a glycosyl hydrolase domain. Sequence analyses revealed *DoVIN2* as a stable, hydrophilic protein lacking a signal peptide or transmembrane region, but possessing 46 phosphorylation sites. Phylogenetic analysis underscored the conservation of plant VINVs during evolution, with *DoVIN2* clustering with this evolutionary lineage. Furthermore, *GFP* expression assays in rice protoplasts localized *DoVIN2* to the cell nucleus. Tissues-specific expression analysis revealed varying levels of *DoVIN2* expression across tissues, with flower exhibiting the highest expression followed by stem, root, and leaf. The *DoVIN2* promoter region contained abiotic stress-responsive elements. Under cold stress, *DoVIN2* expression increased, accompanied by soluble sugar content, indicating its involvement in polysaccharide accumulation and cold stress response. Conversely, *DoVIN2* expression exhibited a negative correlation with the duration of drought stress, implying its diverse roles in responding to cold and drought stress through distinct signaling pathways. Additionally, in silico protein-protein interaction network data revealed that *DoVIN2* interacts with enzymes implicated in saccharometabolism. These findings suggest that *DoVIN2* plays a crucial role in abiotic stress response by regulating the expression of enzyme genes, thereby enhancing *D. officinale*'s tolerance to adverse conditions. Overall, this study provides valuable insights into the function of *DoVIN2* and lays a foundation for investigation into *D. officinale*'s response to abiotic stress.

Key words: *DoVIN2*; Vacuolar invertase; Gene expression; Abiotic stress; Sucrose metabolism.

Introduction

Dendrobium officinale (*D. officinale*), also known as *Dendrobium catenatum*, is a perennial herbal plant native to China and classified under the Orchidaceae family. Highly esteemed for its medicinal properties, it is particularly valued for its rich content of polysaccharides, which are associated with various therapeutic effects such as immune enhancement, blood sugar and lipid reduction, tumor suppression, fatigue alleviation, and improvement of intestinal function (Sun *et al.*, 2020; Chen *et al.*, 2021). Sucrose, the primary product of photosynthesis in *D. officinale*, serves as the main form of carbohydrate transportation (Li *et al.*, 2016). Upon transportation from the leaves, sucrose is hydrolyzed and transformed into polysaccharides by enzymes such as sucrose synthase (SUS) and invertase (INV), with INV playing a predominant role in sucrose hydrolysis (Yang *et al.*, 2012; Li *et al.*, 2015).

In higher plants, the INV gene family is diverse and primarily categorized into three types based on optimal pH values, solubility, and subcellular localization: cytoplasmic invertase (CINV), cell wall invertase (CWINV), and vacuolar invertase (VINV) (Sergeeva *et al.*, 2006; Ruan *et al.*, 2010; Xu *et al.*, 2019). Among these, CINV is classified as a neutral/alkaline invertase (NINV), while CWINV and VINV are categorized as acid invertases (AINV), also known as β -fructofuranosidase, due to their ability to hydrolyze sucrose and other β -fructose oligosaccharides

(Ruan *et al.*, 2010). Notably, VINV plays a crucial role in plant cell osmotic regulation, tissue and organ differentiation, hormone responses, and stress resistance processes (Verhaest *et al.*, 2006; Jain *et al.*, 2017). The number of VINV genes varies across plant species, and their temporal and spatial expression patterns profoundly impact photosynthate transportation, accumulation, and crop yield (Sturm, 1996; Liu *et al.*, 2014). For instance, Yao *et al.*, (2014) identified three VINVs in cassava (*Manihot esculenta*), yet only two displayed functionalities. In rice (*Oryza sativa*), two VINVs, *OsVIN1* and *OsVIN2*, were identified, each exhibiting distinct expression patterns (Ji *et al.*, 2005). *OsVIN1* displayed high expression levels during heading and flowering stages, while *OsVIN2* exhibited high expression levels from 3 days before heading to 3 days after heading (Ji *et al.*, 2007). The stem sugar content of sweet sorghum showed a negative correlation with VINV expression, indicating VINV's crucial role in regulating stem sugar accumulation (Liu *et al.*, 2013). Additionally, the VINV mutant (*sgs1*) in rice exhibited a reduction in grain size and weight, attributable to diminished cell size in both spikelet hull and endosperm, consequently leading to a decrease in yield (Xu *et al.*, 2019).

Furthermore, VINVs play important regulatory role in promoting plant growth and accelerating the breakdown of sucrose, leading to the accumulation of polysaccharides (Sergeeva *et al.*, 2006; Jain *et al.*, 2017). For instance, overexpression of *CsINV5*, a VINV gene from tea (*Camellia*

sinensis), in *Arabidopsis* was found to promote the elongation of the main root and lateral roots by affecting glucose-mediated auxin signaling (Qian *et al.*, 2018). Conversely, Wang *et al.*, (2019a) observed downregulation of transcripts encoding VINV and 6-phosphofructokinase in the internodes of sugarcane (*Saccharum officinarum*) with high sucrose accumulation. Further studies revealed that peptidyl-prolyl isomerases (*FKBP15-1* and *FKBP15-2*) negatively regulate lateral root development by inhibiting VINV activity (Wang *et al.*, 2019b; Wang *et al.*, 2020a, 2020b). Moreover, VINVs also implicated in responses to various biotic and abiotic stresses (Li *et al.*, 2018; Chen *et al.*, 2019). For example, under drought stress, VINV expression decreases in maize (*Zea mays*) ovaries but can recover through sucrose supplementation, highlighting its role in stress adaptation (McLaughlin & Boyer, 2004). Similarly, high-temperature stress reduced VINV activity in maize kernels, affecting starch synthesis and grain yield (Cheikh & Jones, 2006). Furthermore, VINV is associated with heat tolerant in tomato (*Solanum lycopersicum*) cultivars, where higher VINV activity correlates with enhanced stress resilience (Ruan *et al.*, 2010).

In *D. officinale*, previous studies identified four members of the AINV gene family, including two VINV genes (Liu *et al.*, 2022). Among these, one of the VINV gene, named *DOSAI*, was isolated from *D. officinale* grown in Yunnan (Meng *et al.*, 2017). However, detailed structural and functional characterization of the gene, particularly its response to abiotic stress, remains limited. Therefore, the present study focused on amplifying and characterizing *DOSAI* (now referred to as *DoVIN2* in this study) from the *D. officinale* Danxia cultivar using homologous cloning techniques. Through bioinformatics analysis and expression profiling, the study aimed to elucidate the tissues-specific expression and stress-response characteristics of *DoVIN2*, providing insights into its regulatory mechanisms in polysaccharide synthesis and abiotic stress response.

Materials and Method

Plant material, growth conditions and treatment: The *D. officinale* Danxia cultivar was obtained from the *Dendrobium* herb at the Engineering Technology Development Center in Shaoguan, China. Capsules were surface-disinfected, and seeds were sown in half-strength Murashige and Skoog (MS) medium (Sigma-Aldrich, St. Louis, MO, USA) supplemented with 20% potato flour. Seedlings were cultivated aseptically at 25°C ± 1°C with a 12/12-h light/dark cycle and 60%–70% relative humidity in a growth chamber at Shaoguan University (Shaoguan, China). Subculturing occurred every 2 months until seedlings reached a height of 5–6 cm (approximately 6 months old), followed by various treatments. Each treatment comprised six leaves pooled from six separate seedlings, with experiments performed in triplicate.

For simulated drought stress treatment, seedlings were cultured on solid 1/2 MS medium supplemented with 20% polyethylene glycol (PEG) 6000 for 24 hours. Control seedlings were cultured on solid 1/2 MS medium without PEG. For cold stress treatment, seedlings grown on solid 1/2 MS medium were transferred to a growth chamber maintained at a temperature of 4 ± 1°C for 24 hours. Control seedlings were maintained under normal growth

conditions. Then all treated leaves were harvested at 0, 1, 3, 6, 9, 12, and 24 hours post-treatment for expression analysis. Seedlings were collected at 0, 12, 24 and 48 h post-treatment to assess soluble sugar content. Moreover, leaf, stem, root, and flower samples were obtained from *D. officinale* plants during the flowering stage and subjected to identical treatment protocols. Samples were collected in triplicate for biological replication. Subsequently, all samples were promptly flash-frozen in liquid nitrogen and stored at –80°C for subsequent experiments.

RNA isolation, cDNA synthesis, identification and cloning of *DoVIN2*: Total RNA was isolated from *D. officinale* leaves using MiniBEST Plant RNA Extraction Kit (9769, TaKaRa, Japan). RNA concentration and quality were detected using a NanoDrop 600 spectrophotometer (Nano-600, Jiapeng, Shanghai, China) and 1% agarose gel electrophoresis. Subsequently, first-strand cDNA was synthesized using PrimeScript RT Master Mix (RR036A, TaKaRa, Japan).

The cDNA obtained from *D. officinale* leaf samples served as the template for cloning the *DoVIN2* gene. Specific primers (Table 1) were designed using Primer Premier 5.0 software based on the open reading frame (ORF) sequence of the published *DOSAI* gene (GenBank No. KU598852) retrieved from the GenBank database (<https://www.ncbi.nlm.nih.gov/genbank/>). The ORF sequence of *DoVIN2* was amplified via polymerase chain reaction (PCR). Subsequently, the amplified products were purified using a Fast Pure Gel DNA Extraction Mini Kit (AU1701, BioTeke, Beijing, China), subcloned into the pUCm-T vector (B522211, Sangon Biotech, Shanghai, China), and subjected to sequencing by Sangon Biotech (Guangzhou, China).

Analysis of gene structure and protein properties: The exon and intron structures of *DoVIN2* were analyzed using the Gene Structure Display Server 2.0 (<http://gsds.cbi.pku.edu.cn/>) by comparing the relevant coding DNA sequence with genomic DNA (gDNA). The promoter sequences, located 2.0-kb upstream of the start codon of the *DoVIN2* gene, were analyzed using the PlantCARE database (<http://bioinformatics.psb.ugent.be/webtools/plantcare/html/>). The theoretical molecular weight (Mw), isoelectric point (pI), and instability index (II) of the protein were calculated using the ExPasy database (<http://expasy.org/>). The protein domain was analyzed using Conserved Domain Database (<https://www.ncbi.nlm.nih.gov/Structure/cdd/wrpsb.cgi>). Prediction of the secondary and tertiary structures was conducted using the Self-Optimized Prediction Method from Alignment (https://npsa-prabi.ibcp.fr/cgi-bin/npsa_automat.pl?page=npsa_sopma.html) and the ExPasy Swiss-Model (<http://swissmodel.expasy.org/>), respectively. The transmembrane helices and signal peptides were predicted using the Hidden Markov Models Server v2.0 (<https://services.healthtech.dtu.dk/service.php?TMHMM-2.0>) and the SignalP 5.0 Server (<https://services.healthtech.dtu.dk/service.php?SignalP-5.0>). The subcellular localization was predicted using Cell-PLoc 2.0 (<http://www.csbio.sjtu.edu.cn/bioinf/Cell-PLoc-2/>) online tools. Phosphorylation sites were predicted using NetPhos 3.1 Servers (<https://services.healthtech.dtu.dk/service.php?NetPhos-3.1>).

Table 1. The primers used in the study.

Primer name	Primer sequence (5' - 3')	Product size (bp)	T _m (°C)
DoVIN2-F	ATGGCTGAAACGACTGCCTAC	1368	58
DoVIN2-R	TTATGAGAATTGGTATGCGTG		
DoVIN2-GFP-F	TCTCTCTCGAGCTTTTCGCGAGCTCATGCTCTACACCGGTTCCAC	1365	58
DoVIN2-GFP-R	TCGCCCTTGCTCACCATGGATCCTGAGAATTGGTATGCGTGTTC		
qDoVIN2-F	CGAGCAGACTGCCACATAC	153	60
qDoVIN2-R	AGCATCTCGCCGTGAAGAAC		
qDoACTIN-F	CCCTACCTCCTACCTCTGCG	150	60
qDoACTIN-R	GCAAACCCAGCCTTCAACAT		

Phylogenetic analysis and protein–protein interaction network: The VINV protein sequences of *Arabidopsis thaliana* (AtVIN) and other plants, including eight eudicots: *Solanum lycopersicum* (SlVIN), *Capsicum annuum* (CaVIN), *Vitis vinifera* (VvVIN), *Beta vulgaris* (BvVIN), *Glycine max* (GmVIN), *Medicago truncatula* (MtVIN), *Solanum tuberosum* (StVIN), and *Citrus grandis* (CgVIN); and six monocots: *Oryza sativa* (OsVIN), *Sorghum bicolor* (SbVIN), *Zea mays* (ZaVIN), *Ananas comosus* (AcVIN), *Musa acuminata* (MaVIN), *Hordeum vulgare* (HvVIN), were retrieved from the TAIR database (<https://www.arabidopsis.org/>) and the Ensembl Plants database (<https://plants.ensembl.org/info/data/ftp/index.html>) for multiple sequence alignment and phylogenetic analysis. DNAMAN software (version 6.0) was employed for multiple sequence comparisons, while phylogenetic analysis was conducted using MEGA 11 with the neighbor-joining algorithm and bootstrap testing with 1000 replicates. The potential interaction proteins of DoVIN2 were aligned using the latest STRING v11.5 database (<https://cn.string-db.org/>) to predict their relationships.

Subcellular localization of DoVIN2: The *DoVIN2* coding sequence, excluding the termination codon, was inserted into the pC1300s vector using specific primers (Table 1) containing the cauliflower mosaic virus (CaMV) 35S promoter and a *GFP* gene, resulting in the generation of the *35S-DoVIN2-GFP* fusion gene. The constructed clone was verified by DNA sequencing performed by Sangon. Mesophyll protoplasts were isolated from fresh leaves of two to three-week-old Nipponbare rice seedlings and transfected with an empty vector (*35S::pC1300s-GFP*) or the constructed *35S::DoVIN2-GFP*. Mesophyll protoplast isolation and transfection procedures were performed following the protocol described by Chen *et al.*, (2006). GFP fluorescence was observed and imaged using a laser scanning confocal microscope (Olympus, Fluoview FV1200).

Expression profiling of DoVIN2 across various tissues and organs: The raw RNA-seq reads from various tissues, including flower buds (SRR4431603), gynostemium (SRR4431596), labellum (SRR4431602), sepal (SRR4431597), leaf (SRR4431601), stem (SRR4431600), white parts of root (SRR4431598), and green root tip (SRR4431599), were obtained from the NCBI Sequence Read Archive for profiling the tissue expression of the *DoVIN2* gene (Zhang *et al.*, 2016). Alignment of reads to the NCBI *Dendrobium* reference genome was performed using the HISAT package (Kim *et al.*, 2015), followed by

calculation and normalization of expression levels as fragments per kilobase of exon per million mapped reads (FPKM). The heat map was generated using the eFP Browser function of TBtools (Chen *et al.*, 2023).

Expression analysis of DoVIN2 under cold stress and PEG treatment conditions: Real-time quantitative reverse transcription–PCR (RT-qPCR) amplification was performed using Taq SYBR® Green qPCR Premix (R0202, LabEAD, China) on an Applied Bio-Rad CFX Connect Real-time System (Bio-Rad, USA). The reaction mixture (20 µL) comprised 10 µL of Taq SYBR® Green qPCR Premix, 0.2 µM each of forward and reverse primers, and 2 µL of cDNA template (equivalent to 50 ng of total RNA). The amplification conditions were as follows: initial denaturation at 95°C for 30 s, followed by 40 cycles of denaturation at 95°C for 10 s, annealing at 58°C for 30 s, extension at 72°C for 30 s, and plate reading at 80°C for 1 s. The reactions were prepared to analyze the expression of the *DoVIN2* gene in different tissues (leaf, root, stem, and flower) and under various treatments (Cold and PEG). The *DoACTIN* gene served as an internal control (Yuan *et al.*, 2020). Each experiment included triplicate reactions, and three biological replicates were performed. The primers used in the RT-qPCR experiments are listed in Table 1. The relative expression levels were calculated using the normalized expression method ($2^{-\Delta\Delta CT}$ method) (Livak & Schmittgen, 2001).

Measurement of total soluble sugar concentration: Total soluble sugar was extracted from the *D. officinale* seedlings using the water extraction and alcohol precipitation method. Subsequently, the soluble sugar content was determined using the phenol-sulfuric acid method, employing ultraviolet spectroscopy with anhydrous glucose as the reference substance at a wavelength of 483 nm. The content was calculated using a standard curve of anhydrous glucose, which exhibited good linearity ($r = 0.9993$), based on the regression equation $y = 3.5696x + 0.0065$.

Statistical analysis

All data were analyzed using either a one-way analysis of variance (ANOVA) or a Student's t-test, with a significance level set at 0.05 in GraphPad Prism v9.5 (GraphPad Software, Inc., Chicago, USA, www.graphpad.com) to determine the differences between values. Three biological replicates were performed for each analysis. The values presented in the figures represent the average of three replicates, with the standard deviation (SD) indicating sample variability.

Results

Isolation of cDNA from the *DoVIN2* and sequence characterization analysis: The full-length cDNA of *DoVIN2* was isolated from *Dendrobium officinale* (*D. officinale*) leaves, revealing an ORF of 1368 bp in length, encoding a protein of 455 amino acids (Fig. 1a). Comparison analysis of the *DoVIN2* gene with the public genomic sequence of *D. officinale* revealed its location on chromosome 8, spanning four introns and three exons (Fig. 1b). Through alignment with the reference sequence, four nucleotide differences were identified, comprising two synonymous substitutions and two nonsynonymous mutations (Fig. 2).

The bioinformatics analysis indicated that *DoVIN2* belongs to the glycoside hydrolase family 32 and contains a conserved glycosyl hydrolase domain (Glyco_32), characteristic of the AINV gene family (Fig. 3a). The *DoVIN2* protein exhibited a theoretical molecular weight of 50.74 kDa, an isoelectric point of 5.32, and a grand average of hydropathicity of 37.87. Furthermore, it was identified as a hydrophilic protein devoid of both transmembrane regions and signal peptides (Fig. 3b). The secondary structure analysis of the *DoVIN2* protein revealed a predominant composition of random coils, constituting 53.41% of the structure, followed by extended strands at 28.35% and alpha helices at 11.43% (Fig. 3c). Its tertiary structure exhibited a striking similarity to beta-fructofuranosidase from *Vanilla planifolia*, with a high sequence identity of 74.39% (Fig. 3d). Additionally, the *DoVIN2* peptide chain contained a total of 46 putative phosphorylation sites, comprising 25 serine (Ser) sites, 14 threonine (Thr) sites, and 7 tyrosine (Tyr) sites (Fig. 3e).

Phylogenetic analysis of the *DoVIN2* protein: To further elucidate the evolutionary relationship between *DoVIN2* in *D. officinale* and that in other species, a comparative analysis was conducted on 23 full-length amino acid sequences from six monocot plant species, along with 20 full-length amino acid sequences from nine eudicot plant species, resulting in a total of 43 VINV proteins (Fig. 4). The results revealed that VINV members from various species clustered into two distinct subgroups within the evolutionary tree based on taxonomic classification. Specifically, all monocot VINV members grouped into the monocot subgroup, whereas all eudicot VINV members formed the eudicot subgroup. This observation indicates a high degree of conservation among plant VINVs throughout evolution. Furthermore, it implies that plant VINVs evolved and executed their biological functions before the divergence of monocot and eudicot plants. Notably, *DoVIN2* was positioned within the monocot subgroup and exhibited close clustering with *MaVIN1* from bananas on a separate branch, suggesting a close relationship and potentially similar biological functions.

Subcellular localization of the *DoVIN2* protein: Accurate subcellular localization of a protein is crucial for its effective execution of biological functions within the cell. Initial subcellular localization prediction results suggested that *DoVIN2* might be localized to the vacuole. However, fluorescence microscopy analysis of rice mesophyll

protoplasts harboring the 35S::DoVIN2-GFP fusion protein revealed fluorescence exclusively within the nucleus, contrasting with the ubiquitous distribution observed with 35S::pC1300s-GFP control (Fig. 5). This finding demonstrates the nuclear localization of the *DoVIN2* protein.

Expression analysis of the *DoVIN2* gene across various tissues: The expression profile of the *DoVIN2* gene was performed by reanalyzing RNA-seq data from eight tissues to explore its potential functional role across various tissues in *D. officinale* (Zhang et al., 2016). The relative expression levels of *DoVIN2* varied significantly across different tissues, with the highest expression observed in the flower, particularly in the sepal, gynostemium, flower buds, and labellum, while the lowest expression was detected in the leaf (Fig. 6a). These findings suggest that *DoVIN2* may play a crucial role in the formation and development of reproductive organs in *D. officinale*. RT-qPCR analysis further validated the tissue-specific expression pattern of *DoVIN2* in the Danxia cultivar, with the highest expression observed in the flower, followed by the stem and root, compared to the leaf (Fig. 6b). This indicates the potential importance of *DoVIN2* in the development of floral organs in *D. officinale*.

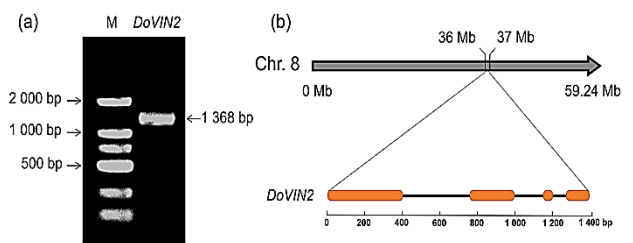


Fig. 1. PCR amplification electrophoresis of *DoVIN2* gene (a), along with its gene structure and chromosome location (b).

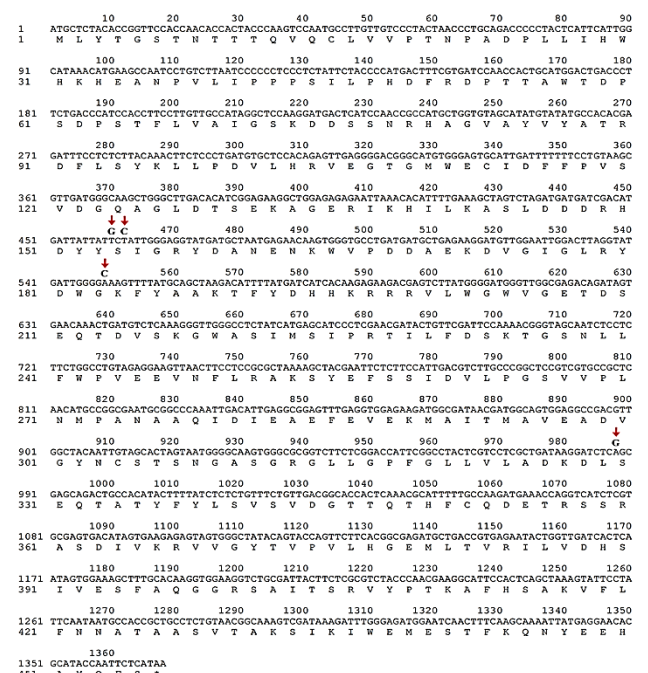


Fig. 2. cDNA sequence of *DoVIN2* gene and its deduced amino acid sequence. The red arrow represents a nucleotide variation between *DoVIN2* and the reference sequences.

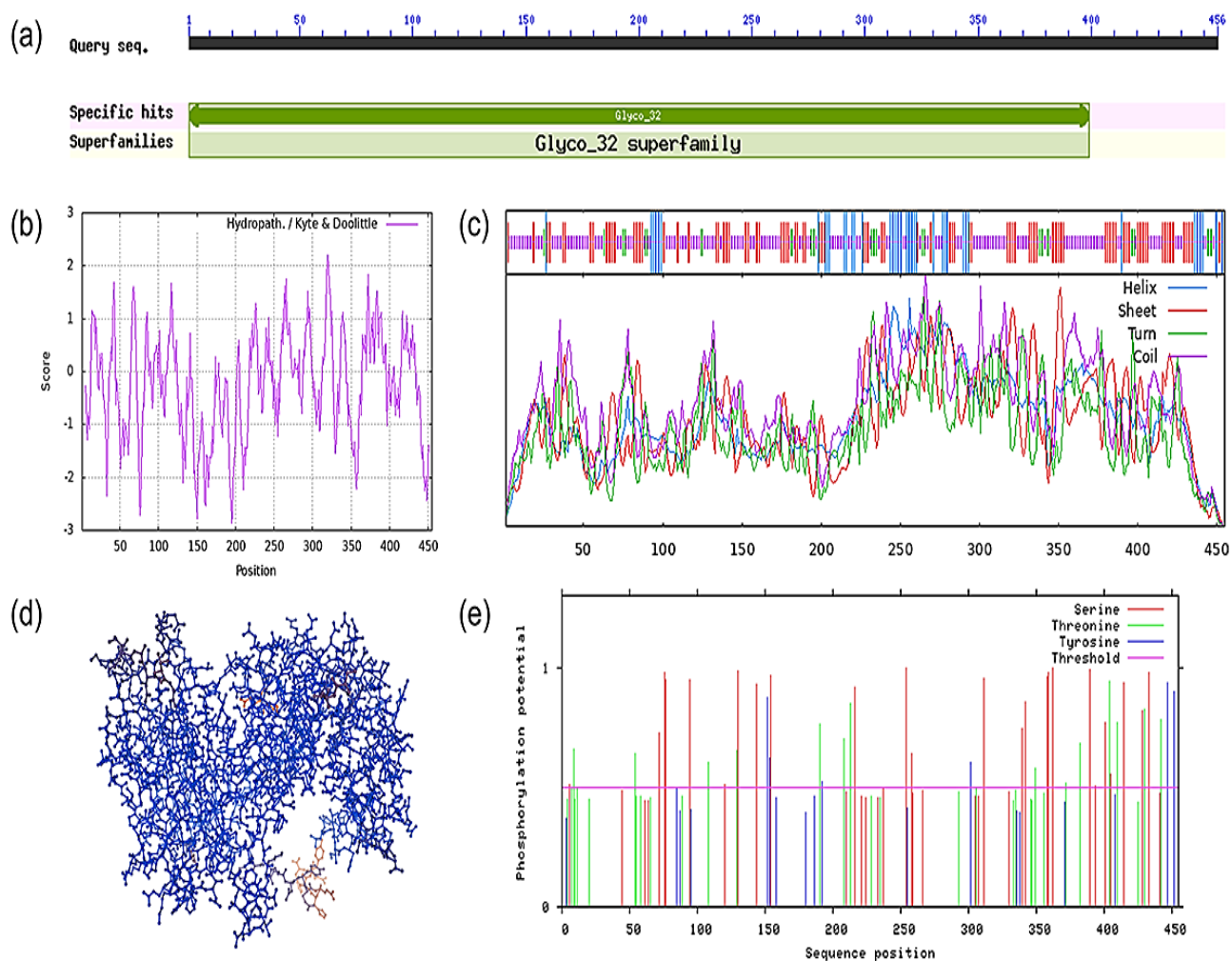


Fig. 3. Prediction and analysis of characteristics of DoVIN2 protein encompass domain organization (a), hydrophobicity (b), secondary structure (c), tertiary structure (d), and phosphorylation sites (e).

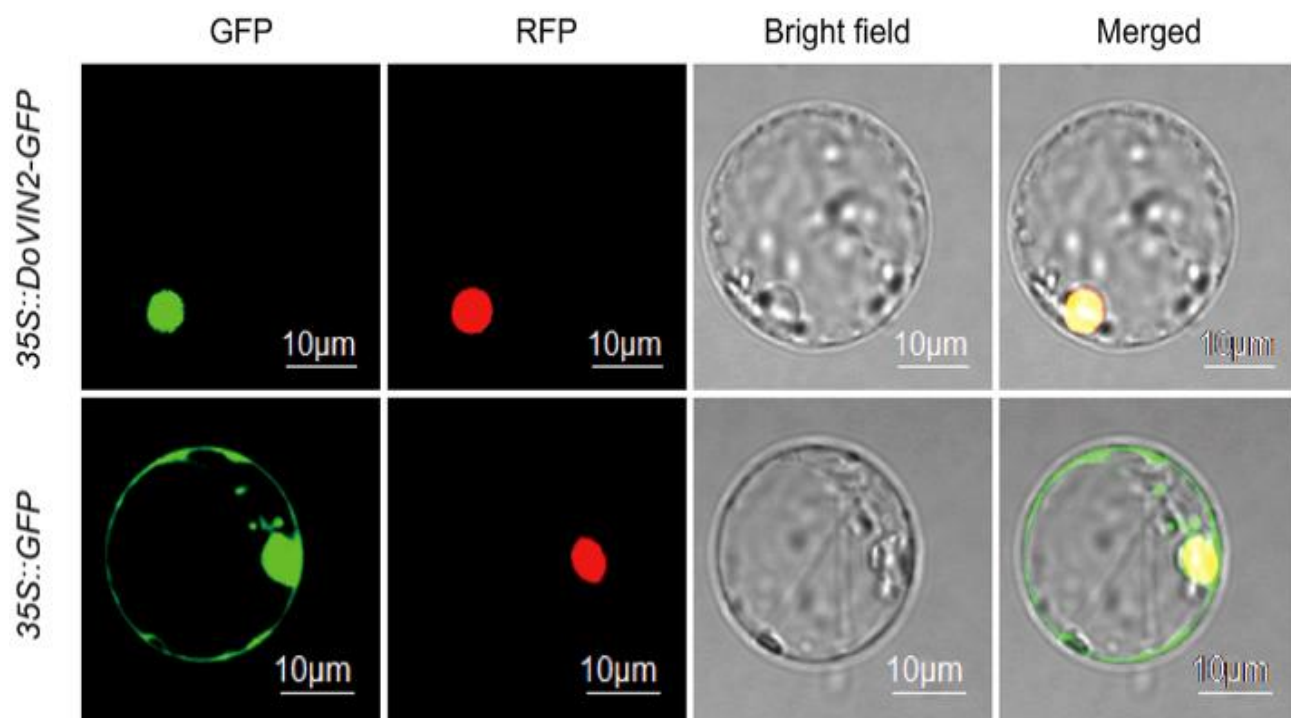


Fig. 5. Subcellular localization of DoVIN2.

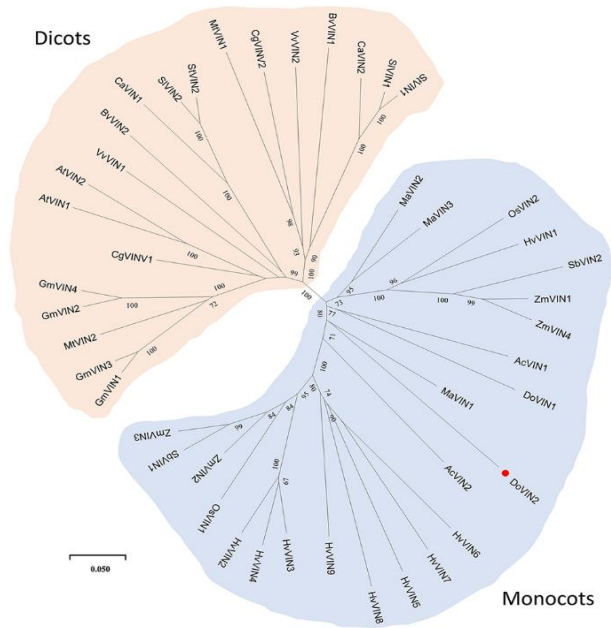


Fig. 4. Phylogenetic analyses of VINV proteins from *Dendrobium officinale* and various species.

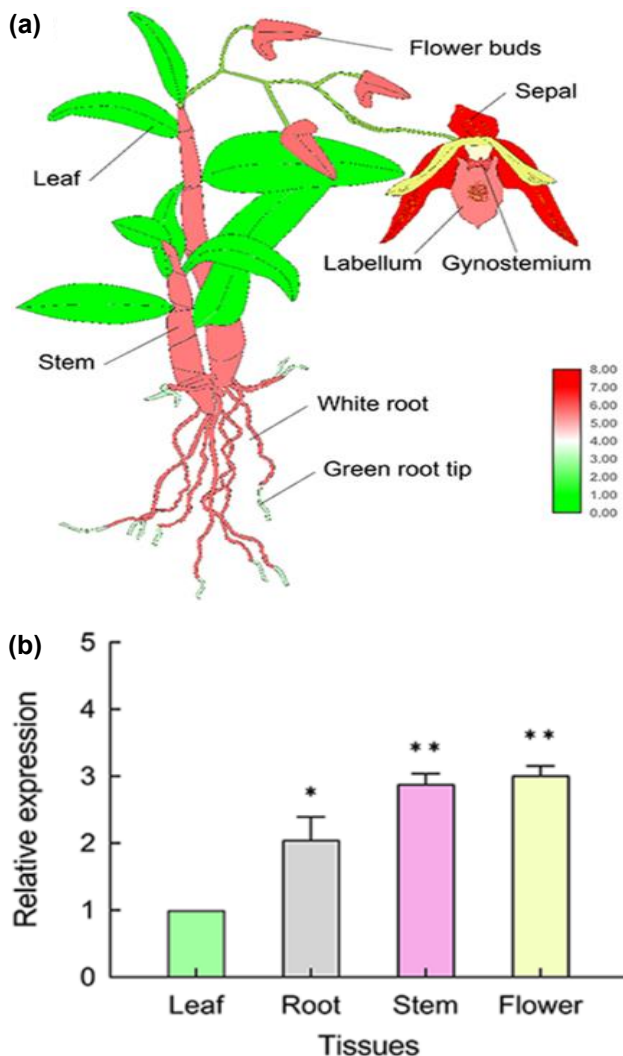


Fig. 6. Tissue-specific expression of *DoVIN2* base on RNA-seq data (a) and RT-qPCR analysis (b). * represents a significant difference at $p < 0.05$; ** indicates a significant difference at $p < 0.01$.

Expression and soluble sugar level analysis of the *DoVIN2* gene under cold and drought stress conditions:

PlantCARE analysis identified the presence of multiple elements responsive to abiotic stress, including low temperature, drought, dehydration, and osmotic pressure, within the 2.0-kb upstream promoter sequences of the *DoVIN2* gene (Table 2). To further elucidate the expression patterns of the *DoVIN2* gene under cold stress and PEG treatment conditions, RT-qPCR analysis was conducted (Fig. 7a). The results revealed a noteworthy upregulation of *DoVIN2* expression in response to cold stress, with a 5.9-fold increase observed after 6 hours compared to its pre-stress levels. Subsequently, the expression levels gradually decreased and eventually returned to the basal level. Conversely, under PEG treatment, *DoVIN2* expression exhibited a declining trend over time, reaching a significantly lower level after 3 hours and persisting until 24 hours of treatment. This indicates a downregulation of the *DoVIN2* gene in response to PEG treatment in *D. officinale*, implying a potential negative regulatory role of *DoVIN2* in response to drought stress.

To explore the relationship between the expression levels of the *DoVIN2* gene and polysaccharide accumulation under cold and drought stress conditions, the soluble sugar content was quantified in *D. officinale* seedlings (Fig. 7b). The findings demonstrated a significant increase in soluble sugar content at 24 and 48 hours compared to the untreated control under both cold stress and PEG treatment. These results suggest that the expression of *DoVIN2* gene varies in response to cold and drought stresses, indicating diverse roles of the *DoVIN2* gene in the plant's response to abiotic stress.

Protein–protein interaction network of *DoVIN2* in *D. officinale*:

The protein–protein interaction network was analyzed using the STRING database to further elucidate the biological function of *DoVIN2* in polysaccharide biosynthesis and abiotic stress response (Fig. 8). The results revealed that *DoVIN2* interacted with several enzymes involved in saccharometabolism, including alpha-galactosidase (α -GAL), beta-glucosidase (BGLU4), sucrose phosphatase (SPP2), sucrose synthase (SUS4 and SUS5), fructokinase (PfkB2 and PfkB5), and hexokinase (HXK1, HXK2, and HXK3) (Table 3). These findings suggest that *DoVIN2* may interact with these enzymes to regulate the expression of related enzyme genes and saccharometabolism pathways during abiotic stress, potentially enhancing polysaccharide accumulation to maintain osmotic homeostasis and alleviate stress-induced damage in plants.

Discussion

In plants, sucrose, a primary product of photosynthesis, functions as a pivotal signaling molecule regulating physiological processes (Zhang *et al.*, 2010; Wang *et al.*, 2017). AINV is a crucial enzyme closely related to sucrose metabolism (Jain *et al.*, 2017; Juárez-Colunga *et al.*, 2018), and several functional VINV genes have been identified across different species, exerting significant impacts on photosynthetic product transport, accumulation, plant morphology, signal transduction, and stress resistance (Chen

et al., 2019; Shen *et al.*, 2018; Xu *et al.*, 2019). In this study, *DoVIN2* was isolated from the *Dendrobium officinale* (*D. officinale*) Danxia cultivar using RT-PCR (Fig. 1), revealing only four nucleotide variations between *DoVIN2*'s ORF and the reference sequence (Fig. 2), suggesting a high conservation of sequence and structure in *DoVIN2*. Phylogenetic analysis indicated that *DoVIN2* clustered with *VINV* members from other monocotyledonous plants, highlighting the conservation of plant *VINVs* during evolution (Shen *et al.*, 2018). Notably, *DoVIN1* and *DoVIN2* were placed within the monocot subgroup but did not branch together, and *DoVIN1* appeared to precede *DoVIN2* (Fig. 4) implying significant divergence among *VINV* gene family members in *D. officinale* during evolution, possibly with distinct regulatory mechanisms, consistent with previous studies on *VINVs* in sweet sorghum and rice (Chi *et al.*, 2020; Deng *et al.*, 2020).

Signal peptides and transmembrane helices are critical for determining protein intracellular localization and secretion (Sinha & Aradhyam, 2019). Bioinformatics analysis predicted that the *DoVIN2* protein lacks both signal peptide and transmembrane regions, suggesting vacuolar localization. However, transient GFP expression analysis in rice mesophyll protoplasts revealed *DoVIN2* localization in the cell nucleus (Fig. 5), consistent with findings by Zheng *et al.*, (2017), where *QUA1*, initially predicted in the Golgi apparatus, was instead localized in the chloroplast, regulating salt and drought stress via chloroplast Ca^{2+} signaling. Given the association between cold stress and organelle function, *DoVIN2* may regulate vacuolar stability through nuclear signal modulation (Cui *et al.*, 2019), possibly facilitating *DoVIN2* transfer from the nucleus to the vacuole to maintain cellular osmotic homeostasis during abiotic stress responses.

Table 2. *Cis*-acting elements analyze in the promoter region of the *DoVIN2* gene.

No.	Regulated element	Motif sequence	Amount	Biological function
1.	LTR	CCGAAA	3	Low-temperature responsiveness
2.	DRE core	GCCGAC	1	Dehydration responsiveness
3.	STRE	AGGGG	4	Osmotic responsiveness
4.	ARE	AAACCA	2	Anaerobic induction element
5.	MYB	CAACAG/CAACCA	3	Environmental stress responsiveness
6.	MYC	CAATTG	1	Environmental stress responsiveness

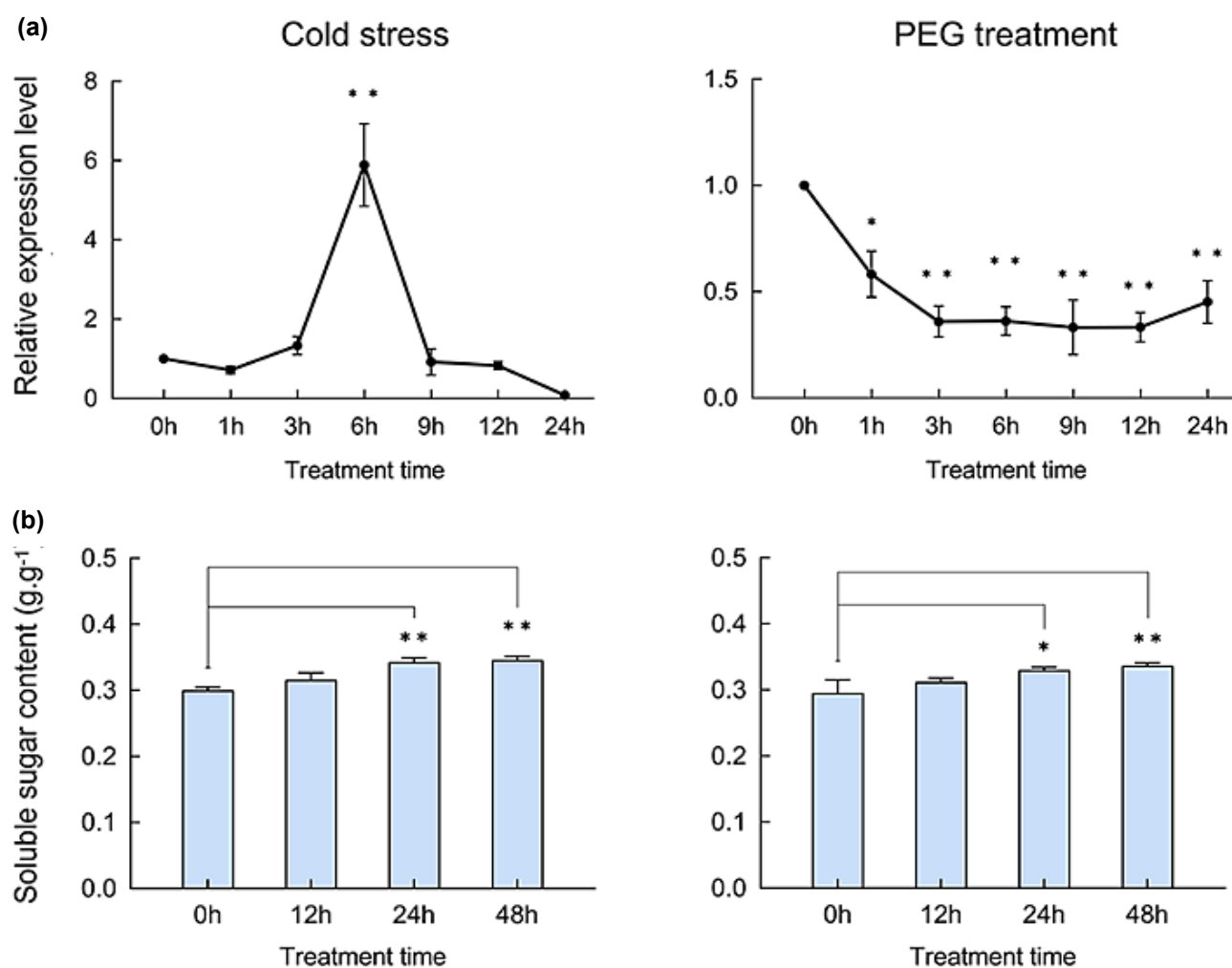


Fig. 7. Expression analysis of the *DoVIN2* gene (a) and measurement of soluble sugar content in *Dendrobium officinale* seedlings (b) under cold stress and PEG treatment. *represents a significant difference at $p < 0.05$; ** indicates a significant difference at $p < 0.01$.

Table 3. Function annotation of DoVIN2-interacting proteins.

Node	Protein string ID	Interaction protein	Registration number	Type of coding protein	EC number
A0A2I0X800	906689.A0A2I0X800	α -GAL	XP_020675455	Alpha-galactosidase	3.2.1.22
BGLU4	906689.A0A2I0WSN2	BGLU4	XP_020699485	Beta-glucosidase 4	3.2.1.21
A0A2I0XID8	906689.A0A2I0XID8	SPP2	XP_020693101	Sucrose phosphatase 2	3.1.3.24
SUS4	906689.A0A2I0XD22	SUS4	XP_020688567	Sucrose synthase 4	2.4.1.13
SUS5	906689.A0A2I0WKD4	SUS5	XP_028552197	Sucrose synthase 5	2.4.1.13
A0A2I0VLJ3	906689.A0A2I0VLJ3	PfkB2	XP_028556705	Fructokinase-2	2.7.1.4
A0A2I0X814	906689.A0A2I0X814	PfkB5	XP_020675418	Fructokinase-5	2.7.1.4
A0A2I0WWJ6	906689.A0A2I0WWJ6	HXX1	XP_020677386	Hexokinase-1	2.7.1.1
HXX2	906689.A0A2I0WYN8	HXX2	XP_020702699	Hexokinase-2	2.7.1.1
HXX3	906689.A0A2I0X5Q3	HXX3	XP_020690061	Hexokinase-3	2.7.1.1

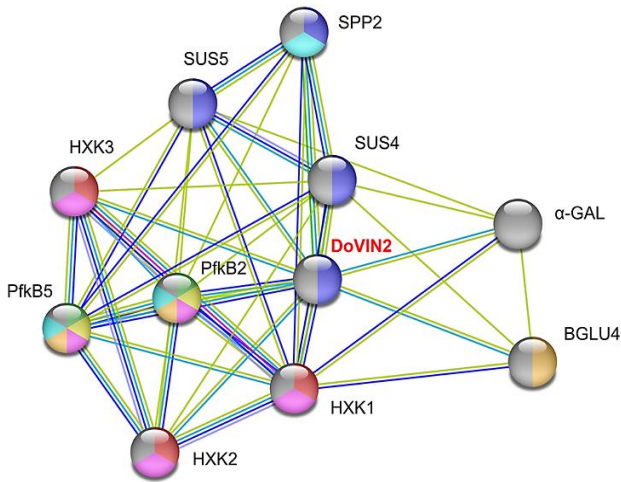


Fig. 8. Protein–protein interaction network of DoVIN2. Node colors signify involvement in diverse biological processes. The edges represent interactions between proteins, with the number of edges indicating the extent of interaction between them.

The tissue-specific gene expression provides valuable insights into gene function, with VINV expression dynamics influencing morphology and growth (Juárez-Colunga *et al.*, 2018; Shen *et al.*, 2018). In *Arabidopsis*, VINV regulates root elongation (Sergeeva *et al.*, 2006), while in sweet sorghum, *SAI-1* is specific to stem (Liu *et al.*, 2013). In our study, *DoVIN2* exhibited significant tissues-specific expression in *D. officinale*, peaking in flower organs (Fig. 6), akin to *LbSAI* in *Lycium barbarum*, underlining their roles in reproductive structure formation (Wang *et al.*, 2014). These findings underscore the conservation and functional diversity of the VINV gene family. Previous studies also link VINV genes to abiotic stress responses (Chen *et al.*, 2019; Liu *et al.*, 2022). In this study, *DoVIN2* was upregulated under cold stress, concurrent with increased soluble sugar concentration (Fig. 7), suggesting its involvement in cold stress response via polysaccharide accumulation. Conversely, *DoVIN2* was downregulated under PEG treatment, despite an increase in soluble sugar concentration, indicating the diverse roles of *DoVIN2* in cold and drought stress responses through distinct signaling pathways. We hypothesize that *D. officinale* employs soluble sugar accumulation as a defense mechanism against abiotic stress. Furthermore, predictive protein–protein interaction analysis revealed that DoVIN2 interacts with enzymes involved in saccharometabolism and polysaccharide synthesis (Fig. 8), indicating its pivotal

role in regulating saccharometabolism during stress. However, the precise regulatory mechanisms warrant further investigation, emphasizing the need for genetic transformation experiments to fully elucidate *DoVIN2*'s functional role.

Conclusion

This study provides evidence that the *DoVIN2* gene may play a significant role in regulating plant growth, in addition to its involvement in the response of *Dendrobium officinale* (*D. officinale*) to abiotic stress. Further experiments involving gene overexpression or knockout are essential for a comprehensive understanding and validation the functions of *DoVIN2*, which will be a focal point of our future research endeavors. Overall, this study establishes a fundamental framework and provides valuable insights into VINV genes in *D. officinale*, laying the groundwork for future investigations.

Acknowledgments

This work was supported by grants from the Foundation for Guangdong Basic and Applied Basic Research (No. 2024A1515013167), the Key Field Projects of Guangdong Provincial Department of Education (No. 2022ZDZX4044 and No. 2024ZDZX2023), the Open Fund of the Guangdong Provincial Key Laboratory of Utilization and Conservation of Food and Medicinal Resources in Northern Region (No. FMR2022002Z), the Shaoguan Science and Technology Program (No. 240823118037510 and No. 230615178031000), and the Key Program of Shaoguan University (No. 9900045704).

References

- Cheikh, N. and R. Jones. 2006. Heat stress effects the sink activity of developing maize kernels grown in vitro. *Physiol. Plant.*, 95(1): 59-66.
- Chen, C., Y. Wu, J. Li, X. Wang, Z. Zeng, J. Xu, Y. Liu, J. Feng, H. Chen, Y. He and R. Xia. 2023. TBtools-II: A “one for all, all for one” bioinformatics platform for biological big-data mining. *Mol. Plant*, 16(11): 1733-1742.
- Chen, L., X. Liu, X. Huang, W. Luo, Y. Long, S. Greiner, T. Rausch and H. Zhao. 2019. Functional characterization of a drought-responsive invertase inhibitor from maize (*Zea mays* L.). *Int. J. Mol. Sci.*, 20(17): 4081.
- Chen, S., L. Tao, L. Zeng, M.E. Vega-Sanchez, K. Umemura and G. Wang. 2006. A highly efficient transient protoplast system for analyzing defence gene expression and protein-protein interactions in rice. *Mol. Plant Pathol.*, 7(5): 417-427.

- Chen, W., J. Wu, X. Li, J. Lu, W. Wu, Y. Sun, B. Zhu and L. Qin. 2021. Isolation, structural properties, bioactivities of polysaccharides from *Dendrobium officinale* Kimura et Migo: a review. *Int. J. Biol. Macromol.*, 184: 1000-1013.
- Chi, Y., K. Wilson, Z. Liu, X. Wu, L. Shang, L. Zhang, H. Jing and H. Hao. 2020. Vacuolar invertase genes *SbVIN1* and *SbVIN2* are differently associated with stem and grain traits in sorghum (*Sorghum bicolor*). *Crop J.*, 8(2): 299-312.
- Cui, X., Y. Wang, J. Wu, X. Han, X. Gu, T. Lu and Z. Zhang. 2019. The RNA editing factor *DUA1* is crucial to chloroplast development at low temperature in rice. *New Phytol.*, 221(2): 834-849.
- Deng, X., X. Han, S. Yu, Z. Liu, D. Guo, Y. He, W. Li, Y. Tao, C. Sun, P. Xu, Y. Liao, X. Chen, H. Zhang and X. Wu. 2020. *OsINV3* and its homolog, *OsINV2*, control grain size in rice. *Int. J. Mol. Sci.*, 21(6): 2199.
- Jain, R., S.P. Singh, A. Singh, S. Singh, R. Kishor, R.K. Singh, A. Chandra and S. Solomon. 2017. Soluble acid invertase (SAI) activity and gene expression controlling sugar composition in sugarcane. *Sugar Tech.*, 19: 669-674.
- Ji, X., W. Van den Ende, L. Schroeven, S. Clerens, K. Geuten, S. Cheng and J. Bennett. 2007. The rice genome encodes two vacuolar invertases with fructan exohydrolase activity but lacks the related fructan biosynthesis genes of the *Pooideae*. *New Phytol.*, 173(1): 50-62.
- Ji, X., W. Van den Ende, A. Van Laere, S. Cheng and J. Bennett. 2005. Structure, evolution, and expression of the two invertase gene families of rice. *J. Mol. Evol.*, 60(5): 615-634.
- Juárez-Colunga, S., C. López-González, N.C. Morales-Elías, J.A. Massange-Sánchez, S. Trachsel and A. Tiessen. 2018. Genome-wide analysis of the invertase gene family from maize. *Plant Mol. Biol.*, 97(4-5): 385-406.
- Kim, D., B. Langmead and S.L. Salzberg. 2015. HISAT: a fast spliced aligner with low memory requirements. *Nat. Methods*, 12(4): 357-360.
- Li, M., T. Chen, T. Gao, Z. Miao, A. Jiang, L. Shi, A. Ren and M. Zhao. 2015. UDP-glucose pyrophosphorylase influences polysaccharide synthesis, cell wall components, and hyphal branching in *Ganoderma lucidum* via regulation of the balance between glucose-1-phosphate and UDP-glucose. *Fung. Genet. Biol.*, 82: 251-263.
- Li, Q., B. Li and S. Guo. 2016. Advance in molecular biology of *Dendrobium* (Orchidaceae). *China J. Chin. Mat. Med.*, 41(15): 2753-2761.
- Li, R., Z. Hou, H. Zou, Y. Wang and X. Liao. 2018. Inactivation kinetics, structural, and morphological modification of mango soluble acid invertase by high pressure processing combined with mild temperatures. *Food Res. Int.*, 105: 845-852.
- Liu, B., Y. Tang, L. Li, Y. Lin, X. Li, B. Bai and Y. Liu. 2022. Identification of acid sucrose invertase gene family in *Dendrobium catenatum* Lindl. and its expression analysis under low temperature. *Jiangsu Agri. Sci.*, 50(24): 33-42.
- Liu, Y., B. Dun, X. Zhao, M. Yue, M. Lu and G. Li. 2013. Correlation analysis between the key enzymes activities and sugar content in sweet sorghum (*Sorghum bicolor* L. Moench) stems at physiological maturity stage. *Aust. J. Crop Sci.*, 7: 84-92.
- Liu, Y., Y. Nie, F. Han, X. Zhao, B. Dun, M. Lu and G. Li. 2014. Allelic variation of a soluble acid invertase gene (*SAI-1*) and development of a functional marker in sweet sorghum [*Sorghum bicolor* (L.) Moench]. *Mol. Breed.*, 33: 721-730.
- Livak, K. and T. Schmittgen. 2001. Analysis of relative gene expression data using real-time quantitative PCR and the 2- $\Delta\Delta C_t$ method. *Methods*, 25(4): 402-408.
- McLaughlin, J.E. and J.S. Boyer. 2004. Sugar-responsive gene expression, invertase activity, and senescence in aborting maize ovaries at low water potentials. *Ann. Bot.*, 94(5): 675-689.
- Meng, H., W. Zhang, B. Lu, Y. Su and C. Xue. 2017. Cloning and expression analysis of soluble acid invertase gene from *Dendrobium officinale*. *J. South China Agric. Univ.*, 38(2): 81-85.
- Qian, W., B. Xiao, L. Wang, X. Hao, C. Yue, H. Cao, Y. Wang, N. Li, Y. Yu, J. Zeng, Y. Yang and X. Wang. 2018. *CsINV5*, a tea vacuolar invertase gene enhances cold tolerance in transgenic *Arabidopsis*. *BMC Plant Biol.*, 18: 228.
- Ruan, Y., Y. Jin, Y. Yang, G. Li and J.S. Boyer. 2010. Sugar input, metabolism, and signaling mediated by invertase: roles in development, yield potential, and response to drought and heat. *Mol. Plant*, 3(6): 942-955.
- Sergeeva, L.I., J.J.B. Keurentjes, L. Bentsink, J. Vonk, L.H.W. Van der Plas, M. Koornneef and D. Vreugdenhil. 2006. Vacuolar invertase regulates elongation of *Arabidopsis thaliana* roots as revealed by QTL and mutant analysis. *Proc. Natl. Acad. Sci. U. S. A.*, 103(8): 2994-2999.
- Shen, L., Y. Qin, Z. Qi, Y. Niu, Z. Liu, W. Liu, H. He, Z. Cao and Y. Yang. 2018. Genome-wide analysis, expression profile, and characterization of the acid invertase gene family in pepper. *Int. J. Mol. Sci.*, 20(1): 15.
- Sinha S. and G.K. Aradhyam. 2019. Identification and characterization of signal peptide of Mitofusin1 (*Mfn1*). *Biochem. Biophys. Res. Comm.*, 509(3): 707-712.
- Sturm, A. 1996. Molecular characterization and functional analysis of sucrose-cleaving enzymes in carrot (*Daucus carota* L.). *J. Exp. Bot.*, 47: 1187-1192.
- Sun, L., X. Chen, C. Wu and S. Guo. 2020. Advances and prospects of pharmacological activities of *Dendrobium officinale* Kimura et Migo polysaccharides. *Acta. Pharm. Sin.*, 55(10): 2322-2329.
- Verhaest, M., W. Lammens, K. Le Roy, B. De Coninck, C.J. De Ranter, A. Van Laere, W. Van den Ende and A. Rabijns. 2006. X-ray diffraction structure of a cell-wall invertase from *Arabidopsis thaliana*. *Acta. Crystallogr. D. Biol. Crystallogr.*, 62(Pt 12): 1555-1563.
- Wang, J., W. Sun, X. Kong, C. Zhao, J. Li, Y. Chen, Z. Gao and K. Zuo. 2020a. The peptidyl-prolyl isomerases *FKBP15-1* and *FKBP15-2* negatively affect lateral root development by repressing the vacuolar invertase *VIN2* in *Arabidopsis*. *Planta*, 252(4): 52.
- Wang, J., T. Zhao, W. Wang, C. Feng, X. Feng, G. Xiong, L. Shen, S. Zhang, W. Wang and Z. Zhang. 2019a. Culm transcriptome sequencing of Badila (*Saccharum officinarum* L.) and analysis of major genes involved in sucrose accumulation. *Plant Physiol. Biochem.*, 144: 455-465.
- Wang, L., M. Chen, F. Zhu, T. Fan, J. Zhang and C. Lo. 2019b. Alternative splicing is a *Sorghum bicolor* defense response to fungal infection. *Planta*, 251(1): 14.
- Wang, L., H. Zhao, Y. Wang, X. Ding and J. Ma. 2014. Cloning and tissues expression analysis of soluble acid invertase gene from *Lycium barbarum* L. *North. Hort.*, n: 86-90.
- Wang, L., Y. Zheng, S. Ding, Q. Zhang, Y. Chen and J. Zhang. 2017. Molecular cloning, structure, phylogeny and expression analysis of the invertase gene family in sugarcane. *BMC Plant Biol.*, 17(1): 109.
- Wang, X., Y. Chen, S. Jiang, F. Xu, H. Wang, Y.Y. Wei and X. Shao. 2020b. *PpINH1*, an invertase inhibitor, interacts with vacuolar invertase *PpVIN2* in regulating the chilling tolerance of peach fruit. *Hort. Res.*, 7: 168.
- Xu, X., Y. Ren, C. Wang, H. Zhang, F. Wang, J. Chen, X. Liu, T. Zheng, M. Cai, Z. Zeng, L. Zhou, S. Zhu, W. Tang, J. Wang, X. Guo, L. Jiang, S. Chen and J. Wan. 2019. *OsVIN2* encodes a vacuolar acid invertase that affects grain size by altering sugar metabolism in rice. *Plant Cell Rep.*, 38(10): 1273-1290.

- Yang, J., H. Meng, S. Yang, W. Zhang, Y. Zha and G. Wen. 2012. Correlation between soluble polysaccharide and sucrose metabolic enzymes in *Dendrobium officinale*. *J. West China Forest. Sci.*, 41: 62-67.
- Yao, Y., X. Wu, M. Geng, R. Li, J. Liu, X. Hu and J. Guo. 2014. Cloning, 3D modeling and expression analysis of three vacuolar invertase genes from cassava (*Manihot esculenta* Crantz). *Molecules*, 19(5): 6228-6245.
- Yuan, Y., J. Zhang, X. Liu, M. Meng, J. Wang and J. Lin. 2020. Tissue-specific transcriptome for *Dendrobium officinale* reveals genes involved in flavonoid biosynthesis. *Genomics*, 112(2): 1781-1794.
- Zhang, B., V. Tolstikov, C. Turnbull, L.M. Hicks and O. Fiehn. 2010. Divergent metabolome and proteome suggest functional independence of dual phloem transport systems in cucurbits. *Proc. Natl. Acad. Sci. U. S. A.*, 107(30): 13532-13537.
- Zhang, G.Q., Q. Xu, C. Bian, W.C. Tsai, C.M. Yeh, K.W. Liu, K. Yoshida, L.S. Zhang, S.B. Chang, F. Chen, Y. Shi, Y.Y. Su, Y.Q. Zhang, L.J. Chen, Y. Yin, M. Lin, H. Huang, H. Deng, Z.W. Wang, S.L. Zhu, X. Zhao, C. Deng, S.C. Niu, J. Huang, M. Wang, G.H. Liu, H.J. Yang, X.J. Xiao, Y.Y. Hsiao, W.L. Wu, Y.Y. Chen, N. Mitsuda, M. Ohme-Takagi, Y.B. Luo, Y. Van de Peer and Z.J. Liu. 2016. The *Dendrobium catenatum* Lindl. genome sequence provides insights into polysaccharide synthase, floral development and adaptive evolution. *Sci. Rep.*, 6: 19029.
- Zheng, Y., C. Liao, S. Zhao, C. Wang and Y. Guo. 2017. The glycosyltransferase QUA1 regulates chloroplast-associated calcium signaling during salt and drought stress in *Arabidopsis*. *Plant Cell Physiol.*, 58(2): 329-341.

(Received for publication 24 April 2024)